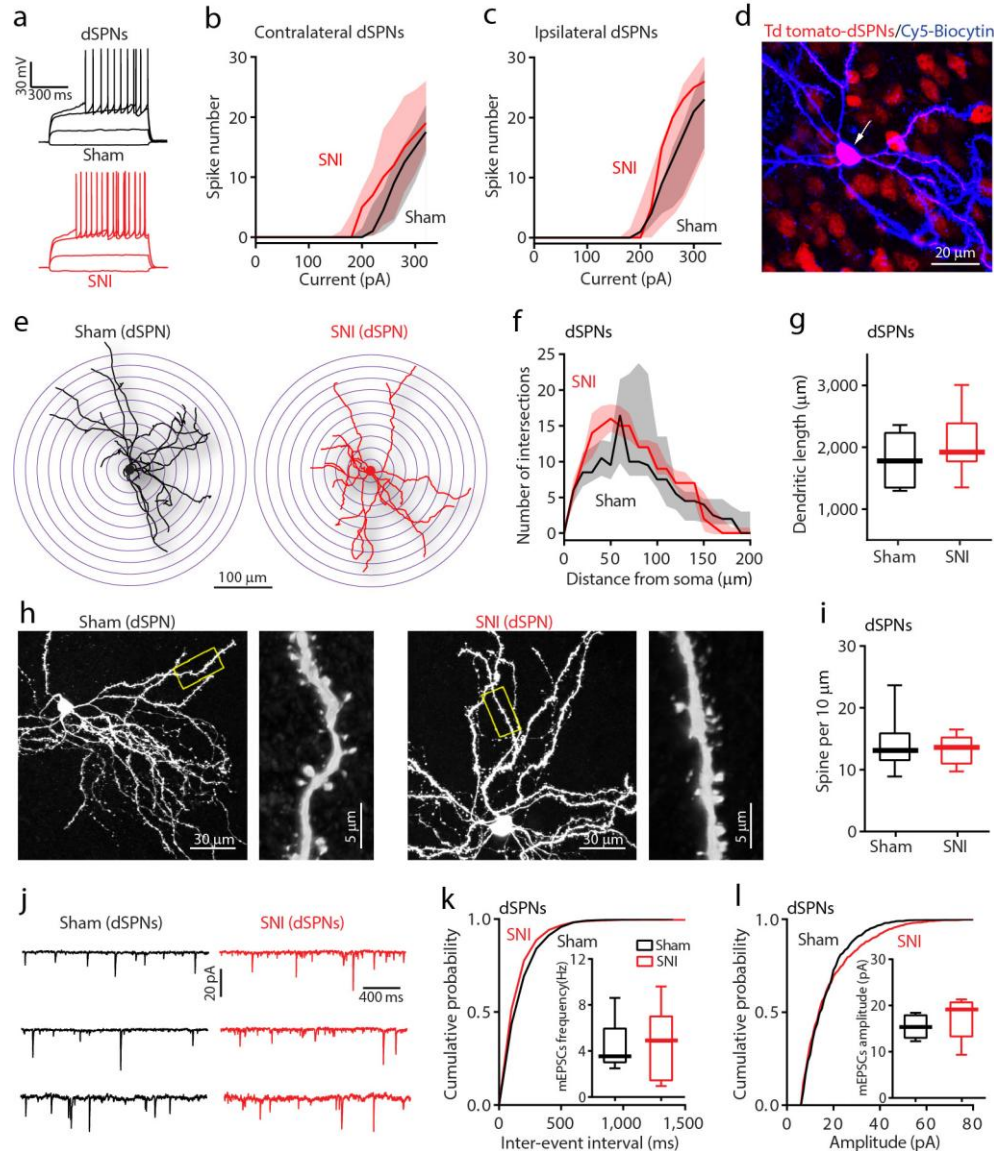


Supplementary Figure 1

The responses to SNI and Sham surgery were similar to in transgenic BAC and wild-type mice.

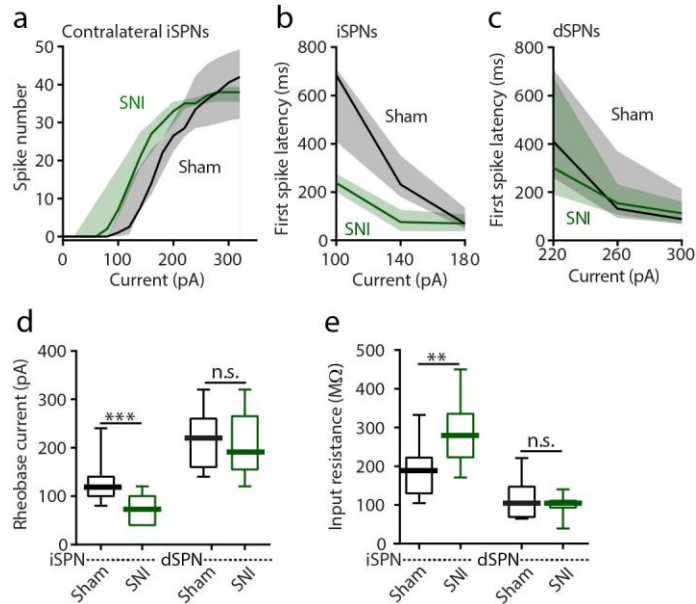
a, In BAC and Wild type (WT) mice, the injured paw VF thresholds of SNI animals were similarly decreased at Day 5 post-surgery (shown as the percentage of pre-surgery; $n = 5$ mice per group, $U = 0$, $p = 0.0079$ for Sham vs SNI in BAC mice; $U = 4$, $p = 0.0873$ for SNI-BAC mice vs SNI-WT mice; $U = 0$, $p = 0.0079$ for SNI vs Sham in WT mice, Mann-Whitney test). Data for **a** are presented as whisker box plots displaying median, lower and upper quartiles, and whiskers representing minimum and maximum of the data. **b**, Sagittal msNAc slice obtained from a BAC transgenic mouse (D, dorsal; V, ventral; R, rostral; C, caudal). **c-d**, No difference in intrinsic excitability was detected in either iSPNs or dSPNs between sham and naïve animals in BAC mice ($n = 11$ neurons from 5 mice per group, $U = 16525$, $p = 0.3464$ for **c** and $U = 16065$, $p = 0.0975$ for **d**, Mann-Whitney test). Data for **c,d** are shown as median with shaded interquartile (quartile 1 to quartile 3).



Supplementary Figure 2

Intrinsic excitability, dendritic morphology and excitatory synaptic connectivity of msNAC dSPNs were not altered in SNI mice.

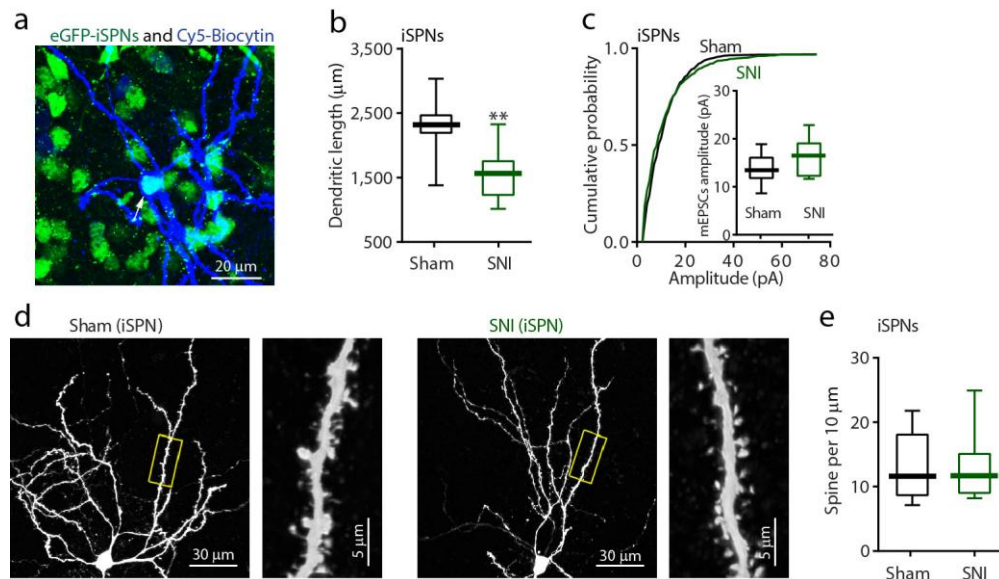
a, Representative traces showing the responses to depolarizing current injections of msNAC dSPNs from Sham ($n = 11$ neurons from 5 mice) and SNI mice ($n = 14$ neurons from 5 mice). **b-c**, In bilateral dSPNs, no difference in intrinsic excitability was detected between Sham and SNI animals (**b**, $n = 6$ neurons from 5 Sham mice and $n = 7$ neurons from 5 SNI mice, $U = 5842$, $p = 0.5717$; **c**, $n = 5$ neurons from 5 Sham mice and $n = 7$ neurons from 5 SNI mice, $U = 5045$, $p = 0.1685$, Mann–Whitney test). **d**, A biocytin filled dSPN was visualized in a msNAC brain slice from a BAC mouse. 20% of biocytin filled dSPNs (5 out of 25) were rejected because dye spillover prevented the assessment of soma integrity. **e-g**, No difference was detectable in dSPN dendritic complexity or dendritic length between Sham and SNI ($n = 10$ neurons from 5 mice per group, $U = 20440$, $p = 0.1934$ for **f**, $U = 34.5$, $p = 0.2546$ for **g**, Mann–Whitney test). **h-i**, dSPNs of SNI and Sham animals had similar spine density ($n = 10$ neurons from 5 mice per group, $U = 45.5$, $p = 0.7541$, Mann–Whitney test). **j-l**, No difference in mEPSC frequency or amplitude was detected in dSPNs of SNI and Sham animals ($n = 7$ neurons from 5 mice per group, Kolmogorov–Smirnov test for representative cumulative probability plots with $D = 0.5490$, $p = 0.2106$ for **k** and $D = 0.2630$, $p = 0.0620$ for **l**; Mann–Whitney test for box plots with $U = 26$, $p = 0.8454$ for **k** and $U = 16$, $p = 0.1883$ for **l**). Data for **b**, **c**, **f** are shown as median with shaded interquartile (quartile 1 to quartile 3); data for **g**, **i**, **k**, **l** are presented as whisker box plots displaying median, lower and upper quartiles, and whiskers representing minimum and maximum of the data.



Supplementary Figure 3

SNI induced an elevation in msNAC iSPN intrinsic excitability.

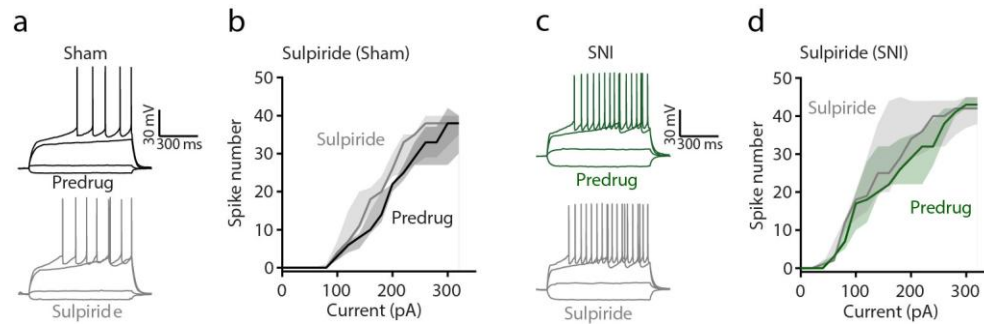
a, iSPN firing was augmented in contralateral msNAC slices ($n = 6$ neurons from 5 Sham mice and $n = 7$ neurons from 5 SNI mice, $U = 5100$, $p = 0.0386$). **b-c**, First-spike latency of iSPNs was shortened in SNI, whereas dSPNs from SNI and Sham had similar first-spike latency ($n = 11$ neurons from 5 mice for each sham group and $n = 14$ neurons from 5 mice for each SNI group, $U = 375$, $p = 0.0005$ for **b** and $U = 675$, $p = 0.8492$ for **c**). **d**, SNI diminished the rheobase current in iSPNs but not in dSPNs ($n = 11$ neurons from 5 Sham mice and $n = 14$ neurons for 5 SNI mice, $U = 19.5$, $p = 0.0008$ for iSPNs and $U = 67.5$, $p = 0.6165$ for dSPNs). **e**, The input resistance of iSPNs was increased by SNI, whereas no difference was detectable in dSPNs ($n = 11$ neurons from 5 Sham mice and $n = 14$ neurons for 5 SNI mice, $U = 27$, $p = 0.0088$ for iSPNs and $U = 68$, $p = 0.6405$ for dSPNs). Data for **a-c** are shown as median with shaded interquartile (quartile 1 to quartile 3); data for **d**, **e** are presented as whisker box plots displaying median, lower and upper quartiles, and whiskers representing minimum and maximum of the data. n.s., not significant ($P > 0.05$), $**P < 0.01$, $***P < 0.001$. Data are analyzed using Mann-Whitney test.



Supplementary Figure 4

SNI had no effect on iSPN spine density.

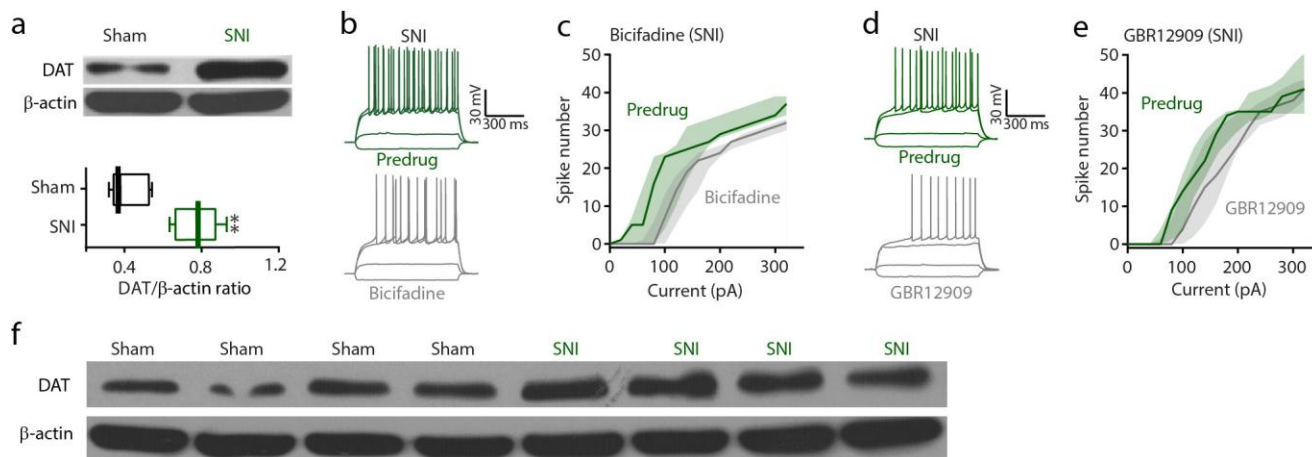
a, A biocytin filled iSPN. Under our staining conditions, 20% of biocytin filled iSPNs (5 out of 25) were rejected because of dye spillover. **b**, SNI reduced total dendritic length in iSPNs ($n = 10$ neurons from 5 mice per group, $U = 11.5$, $p = 0.0022$, Mann-Whitney test). **c**, There was no detectable change in iSPN mEPSC amplitude from SNI and Sham animals ($n = 7$ neurons from 5 mice per group, Kolmogorov-Smirnov test for representative cumulative probability plots with $D = 0.2667$, $p = 0.5107$; Mann-Whitney test for box plots with $U = 14$, $p = 0.2069$). **d-e**, No difference in average spine density was found in iSPN dendrites from SNI and Sham animals ($n = 10$ neurons from 5 mice per group, $U = 48$, $p = 0.8928$). Data are presented as whisker box plots displaying median, lower and upper quartiles, and whiskers representing minimum and maximum of the data, and analyzed using Mann-Whitney test. ****** $P < 0.01$.



Supplementary Figure 5

D2 receptor antagonist sulpiride differentially modulated msNAc iSPN intrinsic excitability in slices from Sham and SNI animals.

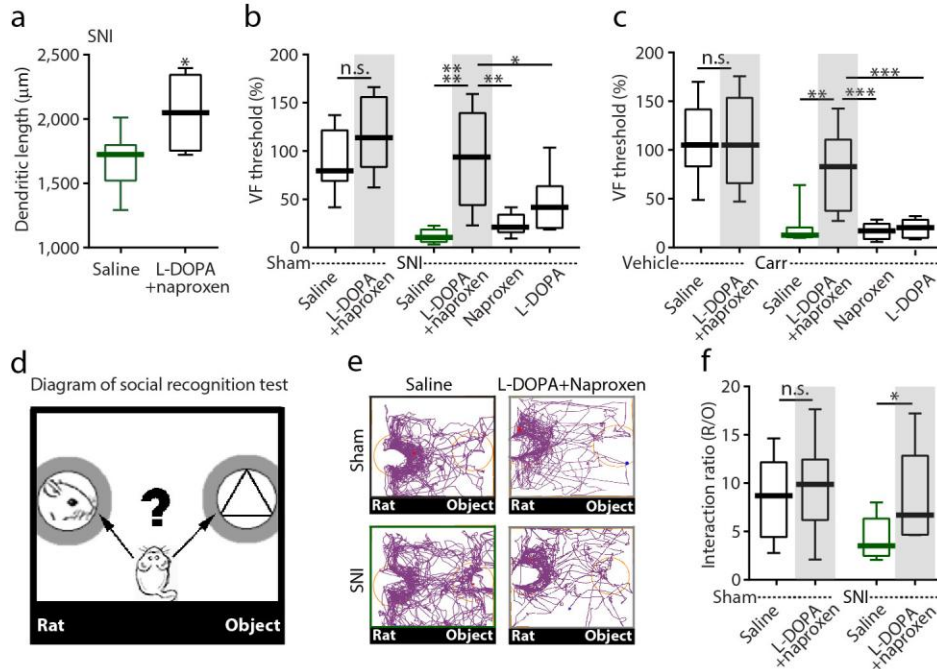
Representative traces showing depolarizing current injections induced firing in msNAc iSPNs from Sham (**a**, $n = 5$ neurons from 5 mice) and SNI animals (**c**, $n = 5$ neurons from 5 mice) before and during sulpiride application. Sulpiride ($5 \mu\text{M}$) increased excitability of iSPNs in Sham (**b**, $W = 1666$, $p < 0.0001$), but had no effect in SNI slices (**d**, $W = 343$, $p = 0.0524$). Data are presented as median with shaded interquartile (quartile 1 to quartile 3), and analyzed using Wilcoxon test.



Supplementary Figure 6

SNI increased the expression of dopamine transporter (DAT) in NAc, and DAT antagonists partially restored iSPN excitability in tissue from SNI mice.

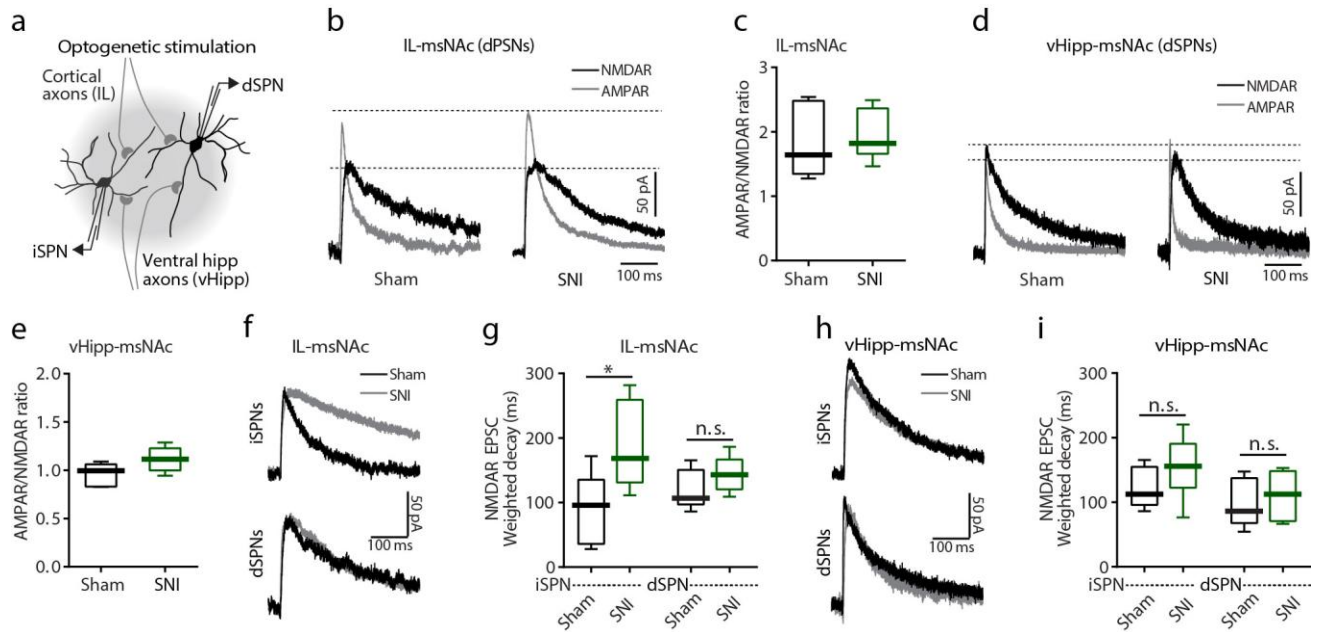
a, Upper: Representative western blot images displaying DAT expression in Sham and SNI ($n = 5$ mice per group). Lower: NAc DAT/ β -actin ratio was significantly higher in NAc from SNI compared with Sham ($U = 0$, $p = 0.0079$, Mann-Whitney test). Data are presented as whisker box plots displaying median, lower and upper quartiles, and whiskers representing minimum and maximum of the data. $**P < 0.01$. **b-e**, Sample traces showing the effect of bicifadine (**b**, $n = 5$ neurons from 5 mice) or GBR12909 (**d**, $n = 7$ neurons from 5 mice) on spikes induced by depolarizing current injections in msNAc iSPNs from SNI animals. Application of DAT antagonist bicifadine ($20 \mu\text{M}$) or GBR12909 ($20 \mu\text{M}$) reduced firing of iSPNs in slices from SNI ($W = -2180$, $p < 0.0001$ for **c** and $W = -2659$, $p < 0.0001$ for **e**, Wilcoxon test). Data are presented as median with shaded interquartile (quartile 1 to quartile 3). **f**, Western blot images showing DAT expression in NAc from all the other 8 animals.



Supplementary Figure 7

L-DOPA and naproxen combined treatment blunted neuropathic and inflammatory tactile allodynia and reversed SNI-induced social ability impairment.

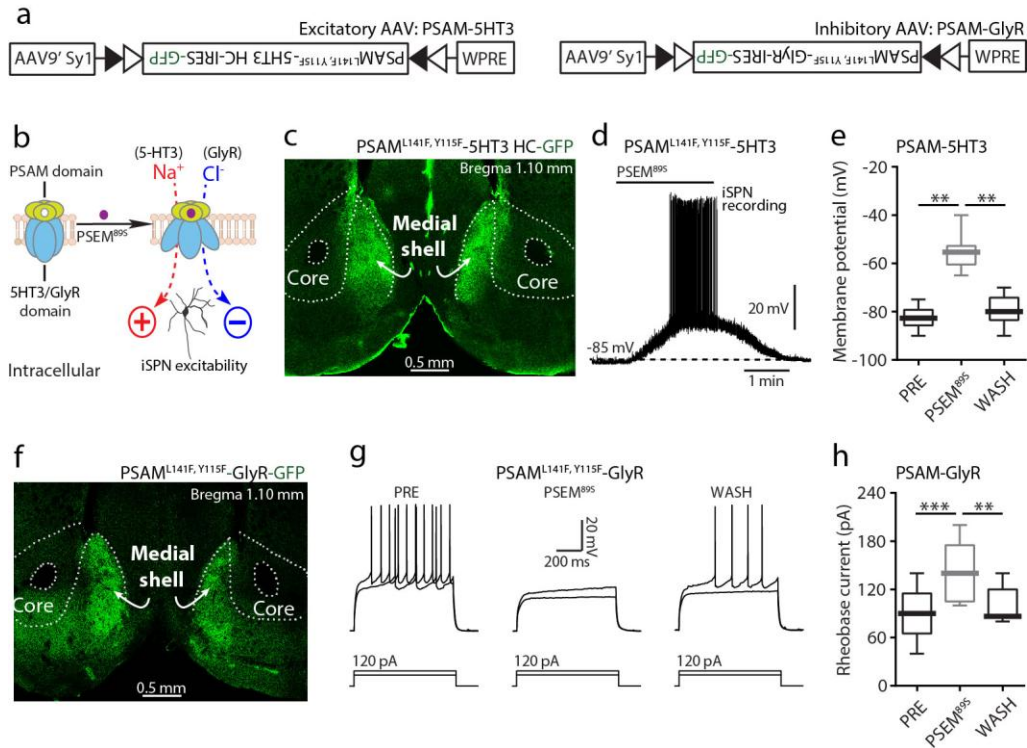
a, L-DOPA and naproxen combined treatment increased dendritic length of iSPNs in SNI ($n = 7$ neurons from 5 mice per group, $U = 8$, $p = 0.0379$). **b-c**, Combined treatment (but not either alone) blocked neuropathic tactile allodynia in SNI rats (**b**, $n = 6$ mice for Combined treatment-Sham, $n = 8$ for Saline-Sham, Saline-SNI and L-DOPA-SNI, $n = 9$ for Combined treatment-SNI and Naproxen-SNI) and reversed inflammatory tactile allodynia induced by carrageenan (Carr) injection into the rat hind paw (**c**, $n = 6$ mice for Saline-Sham and Combined treatment-Sham, $n = 8$ for the other groups) with no effect on tactile response in Sham or vehicle animals (% of pre-surgery, Saline-Sham or -Vehicle vs Combined treatment-Sham or -Vehicle: $U = 13$, $p = 0.1812$ for **b** and $U = 17$, $p = 0.8983$ for **c**; Saline-SNI or -Carr vs Combined treatment-SNI or -Carr: $U = 0$, $p < 0.0001$ for **b** and $U = 3$, $p = 0.0011$ for **c**; Combined treatment-SNI or -Carr vs L-DOPA-SNI or -Carr: $U = 14$, $p = 0.0359$ for **b** and $U = 2$, $p = 0.0006$ for **c**; Combined treatment-SNI or -Carr vs Naproxen-SNI or -Carr: $U = 8$, $p = 0.0028$ for **b** and $U = 1$, $p = 0.0003$ for **c**). Data are shown as the percentage of pre-surgery or pre-saline/carrageenan injection. **d**, Diagram of social recognition test. **e**, Representative tracks of the space explored by animals in each group during the sociability test ($n = 6$ mice for Combined treatment-Sham, $n = 8$ for the other groups). **f**, Combined treatment reversed SNI-induced social ability impairment ($U = 22$, $p = 0.8518$ for Saline-Sham vs Combined treatment-Sham; $U = 13$, $p = 0.0499$ for Saline-SNI vs Combined treatment-SNI). Data are presented as whisker box plots displaying median, lower and upper quartiles, and whiskers representing minimum and maximum of the data, and analyzed using Mann-Whitney test. n.s., not significant ($P > 0.05$), * $P < 0.05$, ** $P < 0.01$, *** $P < 0.001$ and **** $P < 0.0001$.



Supplementary Figure 8

The synaptic strength of IL-msNac dSPNs synapses and vHipp-msNac dSPNs synapses was unchanged by SNI.

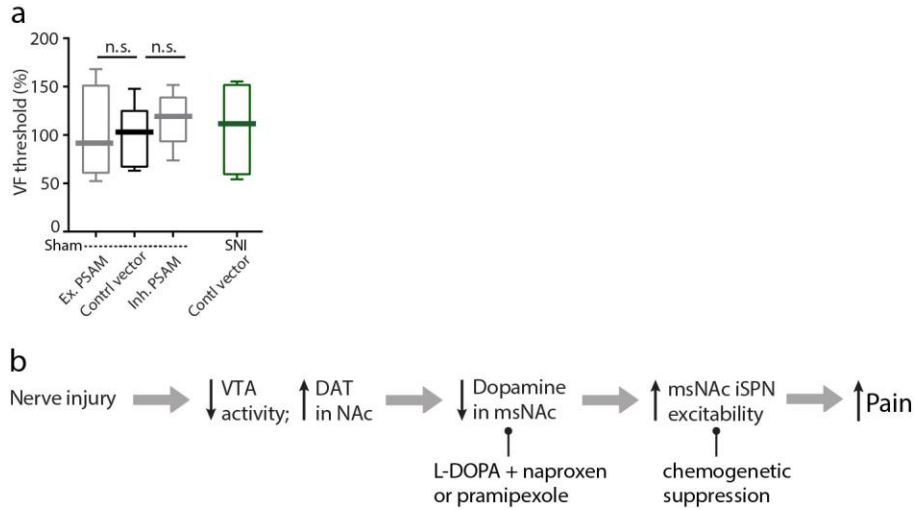
a, Cartoon showing how full-field stimulation with a blue LED was used to assess the strength of each circuit. **b-e**, Representative AMPA and NMDA receptor-mediated currents elicited in the msNac dSPNs with optical stimulation of IL inputs (**b**, $n = 6$ neurons from 5 mice per group) or vHipp inputs (**d**, $n = 5$ neurons from 5 mice per group). At either IL-msNac dSPNs synapses (**c**) or vHipp-msNac dSPNs synapses (**e**), there was no detectable difference in optically evoked AMPA/NMDA receptor currents between SNI and Sham ($U = 15$, $p = 0.6753$ for **c** and $U = 4$, $p = 0.0952$ for **e**). **f-g**, At IL-Nac shell synapses, SNI selectively induced prolonged decay kinetics of NMDAR EPSCs recorded in iSPNs ($n = 6$ neurons from 5 mice per group, $U = 5$, $p = 0.0411$ for iSPNs and $U = 6$, $p = 0.2222$ for dSPNs). **h-i**, At vHipp-msNac synapses, there was no change in decay rate of NMDAR EPSCs recorded in either iSPNs or dSPNs ($n = 6$ neurons from 5 mice for each iSPN group and $U = 10$, $p = 0.2831$ for iSPNs; $n = 6$ neurons from 5 mice for each dSPN group and $U = 11$, $p = 0.8016$ for dSPNs). Optically evoked AMPAR and NMDAR currents were detected in all the recorded SPNs. Data are presented as whisker box plots displaying median, lower and upper quartiles, and whiskers representing minimum and maximum of the data, and analyzed using Mann–Whitney test. n.s., not significant ($P > 0.05$), $*P < 0.05$.



Supplementary Figure 9

PSAM-5HT3 and PSAM-GlyR chimeric ion channels altered msNAc iSPN excitability.

a, Construct for a Cre-dependent recombinant adeno-associated viral (AAV) vector with an inverted bicistronic open reading frame for PSAM^{L141F,Y115F}-5HT3 HC receptors (Left, excitatory PSAM) or for PSAM^{L141F,Y115F}-GlyR receptors (Right, inhibitory PSAM) under control of a FLEX-switch (triangles). **b**, Schematic depicting the construct and the principle of the ligand-gated ion channels expressed by virus of PSAM-5HT3 or PSAM-GlyR. **c**, In AAV-PSAM^{L141F,Y115F}-5HT3 HC-GFP transduced A2A::Cre mice, GFP fluorescence was exclusively expressed in NAc shell ($n = 11$ slices from 11 animals, one slice per animal). **d-e**, representative trace (**d**) and box-plot quantification of membrane potential in iSPNs (**e**) showing that PSEM^{89S} (10 μ M) elicited rapid depolarization and spiking in PSAM^{L141F,Y115F}-5HT3 HC-GFP (excitatory PSAM)-positive iSPN ($n = 10$ neurons from 6 animals, $W = 55$, $p = 0.0020$ for PRE vs PSEM^{89S} and $W = 55$, $p = 0.0020$ for PSEM^{89S} vs WASH). **f**, Image of GFP labeling in NAc shell slice from an A2A::Cre mouse expressing PSAM^{L141F,Y115F}-GlyR-GFP ($n = 14$ slices from 14 animals, one slice per animal). **g-h**, PSAM^{L141F,Y115F}-GlyR (inhibitory PSAM) reversibly reduced the excitatory effect of depolarizing current injections on NAc shell iSPNs in the presence of PSEM^{89S} ($n = 12$ neurons from 7 animals, $W = 66$, $p = 0.0010$ for PRE vs PSEM^{89S} and $W = 68$, $p = 0.0054$ for PSEM^{89S} vs WASH). Expression of the virus reporter GFP was detected exclusively in NAc shell from all the virus injected A2A::Cre mice, and PSEM^{89S} significantly modulated the excitability of all the tested GFP positive neurons in brain slices from the infected mice. In **e,h**, data are presented as whisker box plots displaying median, lower and upper quartiles, and whiskers representing minimum and maximum of the data, and analyzed using Wilcoxon test. ** $P < 0.01$, *** $P < 0.001$.



Supplementary Figure 10

PSAM had no effect on Sham animals.

a, In Sham animals, modulation of msNAc shell iSPNs by excitatory PSAM(Ex. PSAM: PSAM-5HT3) or inhibitory PSAM (Inh. PSAM: PSAM-GlyR) with PSEM^{89S} had no effect on tactile threshold ($n = 5$ mice for Ex. PSAM-Sham, $n = 6$ mice for Control vector-Sham, $n = 6$ for Inh. PSAM-Sham, $n = 7$ for Control vector-SNI; In Sham animals, $U = 15$, $p > 0.9999$ for Ex. PSAM vs Control vector; $U = 11$, $p = 0.3052$ for Inh. PSAM vs Control vector). Data are presented as whisker box plots displaying median, lower and upper quartiles, and whiskers representing minimum and maximum of the data, and analyzed using Mann–Whitney test. **b**, Schematic summarizing msNAc reorganization and pain behavioral changes after nerve injury. n.s., not significant ($P > 0.05$).